
Proceedings Paper:
Kent, JT, Bhattacharjee, S, Hussein, II et al. (2018) Filtering When Object Custody is Ambiguous. In: Proceedings of 2018 21st International Conference on Information Fusion (FUSION). 2018 21st International Conference on Information Fusion (FUSION 2018), 10-13 Jul 2018, Cambridge, UK. IEEE, pp. 1317-1322. ISBN: 978-0-9964527-6-2.

https://doi.org/10.23919/icif.2018.8455593

Filtering when object custody is ambiguous

John T. Kent
Professor, Department of Statistics
University of Leeds
Leeds, UK
j.t.kent@leeds.ac.uk

Shambo Bhattacharjee
PhD Researcher, Department of Statistics
University of Leeds
Leeds, UK
mmsb@leeds.ac.uk

Islam I. Hussein
Aerospace Engineer
Applied Defense Solutions
Columbia, USA
ihussein@applieddefense.com

Weston R. Faber
Aerospace Engineer
Applied Defense Solutions
Columbia, USA
wfaber@applieddefense.com

Moriba K. Jah
Professor, Department of Aerospace Engineering
University of Texas at Austin
Austin, USA
moriba@utexas.edu

***Abstract*—Filtering involves predicting the future state of a space object in orbit about the earth given observations (e.g. angles-only or radar measurements) about its current and past states. The task is simplest when the identity of the object is known. A recently developed "Adapted STructural (AST)" coordinate system enables the task to be carried out in a computationally efficient manner. Propagation for a single state (or a small number of sigma points) can be carried out using Keplerian dynamics or using a numerically more expensive propagator to accommodate perturbation effects. In either case, the uncertainty can be represented in AST coordinates as Gaussian to a high level of accuracy. An Unscented Kalman Filter (UKF) has been developed in this situation; in particular, there is no need to use particle filters.**

However, when object custody is uncertain, i.e. when the latest observation might correspond to two or more objects in a catalog, the filtering task is more complicated. In this case we propose a mixture of Gaussians in AST coordinates to represent the state. The paper will demonstrate the feasibility of this approach.

***Index Terms*—AST coordinates, Unscented Kalman Filter, mixture modeling**

I. Introduction

Uncertainty propagation is a fundamental issue in orbital mechanics for the purpose of object tracking and association problems. For example, Junkins, Akella, and Alfriend [2] studied nonlinear characteristics of the propagated uncertainty under different coordinate systems. They used a Monte Carlo simulation based approach. Park and Scheeres [8] used a mixture (hybrid approach) of a simplified dynamic system (SDS) model and the state transition tensor (STT) model to propagate and model the uncertainty. Vittaldev, Russell and Linares [9] proposed a mixture of polynomial chaos expansion and Gaussian Mixture Models (GMM). Horwood and Poore [4] proposed a Gauss von Mises (GVM) filter. Further, the paper by Hintz [10] provides a concise summary on different coordinate systems. However, these papers mainly used a fixed coordinate system to perform uncertainty analysis.

The problem of space debris tracking can be viewed as an example of Bayesian filtering [1]. Examples of such filters include the classic Kalman filter, together with nonlinear variants such as the extended and unscented Kalman filters, and the computationally more expensive particle filters. We have shown in earlier work that with a careful choice of coordinate system, the uncertainty in the space debris tracking problem can often be formulated in terms of a multivariate normal distribution [5]. Hence when object custody is not in doubt, filtering can be carried out using the Unscented Kalman Filter (UKF) [6]. The purpose of this paper is to extend the analysis to the setting where object custody is ambiguous, using a mixture of multivariate normal distributions.

Up to perturbation effects, an object in orbit around the earth follows an elliptical path. The simplest way to describe the orbit is in terms of Cartesian coordinates (more specifically, Earth-Centered Inertial or ECI coordinates), a six-dimensional state vector for the position and velocity of the object. However, even if the initial uncertainty of the state is normally distributed, following the orbital path for several periods into the future leads to a propagated uncertainty which is distinctly non-normal [2], [3]. The other ingredient in the filtering problem is a set of measurements, taken here to be a set of directions at successive times seen by an observer on the surface of the earth.

In general, the filtering problem is simplest when the joint distribution of the state vector and the observation vector is normally distributed. To achieve this goal, we have introduced in earlier work [5] an "Adapted STructural (AST)" coordinate system to describe the orbiting object. AST coordinates are essentially a type of tangent coordinates to represent the uncertainty in a point cloud about a "central state". The AST coordinate system contains 6 coordinates:

(a) three coordinates to describe an ellipse in a 2-dimensional plane,
(b) two coordinates to describe the normal direction to the elliptical plane, and
(c) one coordinate, the mean anomaly, to describe the location of the object along the ellipse. If we keep track of the winding number (thus turning an *angle* into a *real number*), then the unwrapped mean anomaly is approximately

normally distributed, even under substantial dispersion.

AST coordinates have been defined and studied in some of our earlier papers, especially [1], [5]. One purpose of the current paper is to make their definition more explicit and to confirm their good properties under more extreme initial conditions. The second purpose is to demonstrate the usefulness of AST coordinates when object custody is ambiguous.

Ambiguity in custody occurs when an angles-only observation at a particular time say t_0, can be associated with the states for two or more objects in a catalog or library. For each object in the catalog, there is a predicted state and associated uncertainty at time t_0. The corresponding predicted value for the angles-only position and associated uncertainty can be represented by a point cloud or by a probability density function, typically following an approximate bivariate normal distribution tangent to the unit sphere.

For instance, suppose an angles-only observation $\boldsymbol{x}$ (a unit vector in $\mathbb{R}^3$) may be associated with one of J possible objects in a catalog, with densities $f_j(\boldsymbol{x}),\ j = 1, \ldots, J$. The maximum likelihood rule for discriminant analysis says to allocate $\boldsymbol{x}$ to the population for which $f_j(\boldsymbol{x})$ is largest. Further, if we assume each population has equal prior probability, then the posterior probability that $\boldsymbol{x}$ comes from population j is

$$p_j(\boldsymbol{x}) = \frac{f_j(\boldsymbol{x})}{\sum_{j'=1}^{J} f_{j'}(\boldsymbol{x})}, \quad j = 1, \ldots, J.$$

Fig 1 illustrates some of the issues that can arise. Assume a library of two objects (A and B) and three potential observations (1,2 and 3).

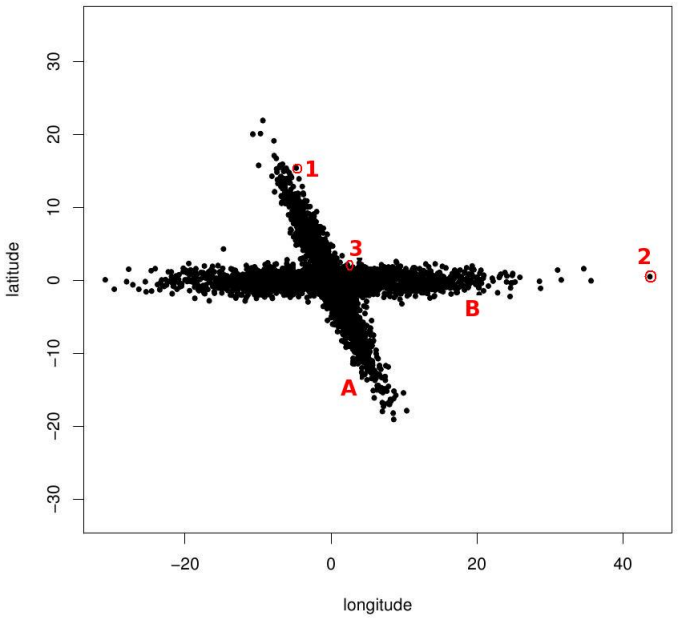

Fig. 1. Two overlapping distributions A and B for the angles-only part of a state vector. The distributions are represented by point clouds in the tangent plane to the unit sphere in terms of latitude and longitude in degrees. In addition three possible observations, labeled 1,2,3, have been highlighted.

Point 1 lies in the main body of the distribution for object A, but not for object B. Hence the posterior probability that point 1 comes from object A is large. Point 2 is more closely associated with B than A, but lies far enough from B that is might be considered incompatible with either object. Point 3 lies midway between the two principal axes, but is close enough to the common mode to be compatible with both distributions. In particular, the posterior probabilities will be nearly equal.

II. AST COORDINATES

Before describing the construction of AST coordinates, it is helpful to recall some standard results from the orbital mechanics [7]. The cross product of $\boldsymbol{x}(t)$ and $\dot{\boldsymbol{x}}(t)$ is called the "specific angular momentum vector" and often represented using the alphabet "$\boldsymbol{h}$". Let $\boldsymbol{n}$ represent the unit vector proportional to $\boldsymbol{h}$. Other standard notation includes r for the altitude at time t, $\boldsymbol{e}$ for the eccentricity vector, e for the eccentricity, r_p and r_a for the radius from perigee and apogee respectively, a for the semi-major axis, b for the semi-minor axis and finally T for the orbital time period. These quantities are given by

$$\begin{aligned}
&\boldsymbol{h} = \boldsymbol{x}(t) \times \dot{\boldsymbol{x}}(t), \quad h = \sqrt{\boldsymbol{h} \cdot \boldsymbol{h}}, \\
&\boldsymbol{n} = \boldsymbol{h}/h, \quad r = \sqrt{\boldsymbol{x}(t) \cdot \boldsymbol{x}(t)}, \\
&\boldsymbol{e} = \frac{1}{\mu}(\dot{\boldsymbol{x}}(t) \times \boldsymbol{h} - \mu \frac{\boldsymbol{x}(t)}{r}), \quad e = \sqrt{\boldsymbol{e} \cdot \boldsymbol{e}}, \\
&r_p = \frac{h^2}{\mu}\frac{1}{1+e}, \quad r_a = \frac{h^2}{\mu}\frac{1}{1-e}, \\
&a = \frac{1}{2}(r_p + r_a), \quad b = \frac{a}{\sqrt{1-e^2}}, \quad T = \frac{2\pi}{\sqrt{\mu}} a^{3/2},
\end{aligned}$$

where μ is the standard gravitational constant. Under Keplerian dynamics (i.e. no perturbation effects), apart from r all these parameters are time invariant.

The standard coordinate systems to represent the state of an orbiting object include the following:

- **Cartesian-ECI:** A state is represented by a three-dimensional position vector and a three-dimensional velocity vector.
- **Keplerian orbital elements:** A state is the represented using the semi-major axis (a), eccentricity (e), inclination (i), RAAN (Ω), argument of perigee (ω) and wrapped true anomaly (M_0).
- **Equinoctial orbital elements:** A state is represented using $a,\ h = e\sin(\Omega + \omega),\ k = e\cos(\Omega + \omega),\ p = \tan(i/2)\sin(\Omega),\ q = \tan(i/2)\cos(\Omega)$ and $\lambda = \Omega + \omega + M_0$.

Next we describe the construction of AST coordinates. This task requires care because the purpose of AST coordinates is to describe the uncertainty in the state of an orbiting object. Suppose uncertainty is described in terms of a point cloud of possible states $(\boldsymbol{x}_j(t), \dot{\boldsymbol{x}}_j(t))$, for $j = 1, \ldots, N$ where N is a large number of possible states. It should be emphasized that the point cloud is only for visualization purposes. For analytic work, the point clouds will be approximated by multivariate

normal distributions and summarized by a collection of sigma points.

Suppose that a "central state" $(\boldsymbol{x}_c(t), \dot{\boldsymbol{x}}_c(t))$ sitting near the middle of the point cloud at time $t = 0$ has been highlighted. The central state will be used as a "base" for our coordinate system about which certain "tangent coordinates" will be constructed.

There are several steps in the construction of AST coordinates. During the construction, it will be helpful to let $Q(\boldsymbol{w})$ denote the 3×3 rotation matrix which takes $\boldsymbol{w}$ to the north pole $[0, 0, 1]^T$ and which keeps the cross product fixed, $Q(\boldsymbol{w})\boldsymbol{u} = \boldsymbol{u}$, where $\boldsymbol{u} = \boldsymbol{w} \times [0, 0, 1]^T$.

(a) Rotate the unit normal vector of the central configuration $\boldsymbol{n}_c$, say, to the north pole. Let $R_{1c} = Q(\boldsymbol{n}_c)$ be the desired rotation and use dashed notation

$$\boldsymbol{x}'_c(t) = R_{1c}\boldsymbol{x}_c(t), \quad \boldsymbol{x}'_j(t) = R_{1c}\boldsymbol{x}_j(t), \quad j = 1, \ldots, N$$

to denote the rotated central state and the rotated point cloud at time t..

(b) The normal directions of the rotated point cloud will lie near the north pole so that the first two elements, of $\boldsymbol{n}'_j = [n'_{j1},\ n'_{j2}, n'_{j3}]^T$ will be close to 0. The first two elements $n'_{j1},\ n'_{j2}$ are two of the AST coordinates.

(c) Let $R_{2j} = Q(\boldsymbol{n}'_j)$ be the rotation taking each dashed normal vector $\boldsymbol{n}'_j$ in the point cloud to the north pole. This will be a small rotation and is determined by the two elements $n'_{j1},\ n'_{j2}$. Use double-dashed notation $\boldsymbol{x}''_j(t) = R_{2j}\boldsymbol{x}'_j(t)$ to denote the double rotated states. The purpose of these second rotations is to ensure that all of the orbital planes are the same as one another (namely, the horizontal plane).

(d) Finally, after rotation by R_{1c} and R_{2j}, let δ''_j denote the angle of perigee of the elliptical orbit in the horizontal plane for the jth state in the point cloud, measured relative to the positive X-axis.

(e) The final AST coordinate is a version of the mean anomaly. The mean anomaly is usually defined in terms of the angular position of the orbiting object measured with respect to perigee. Here, in double-dashed coordinates, the mean anomaly is defined in terms of the angular position of the orbiting object measured with respect to the positive X-axis, and denoted $\xi''_j(t) \mod 2\pi$, say. Further, although the (wrapped) mean anomaly is usually treated as an *angle*, it is also helpful to consider an unwrapped version for which $\xi''_j(t)$ is treated as a *number* (so $\xi''_j(t)$ is an increasing real-valued continuous function of $t \geq 0$). This unwrapped mean anomaly records both the angular position of the object along its orbit, plus the whole number of orbits completed.

In summary, the six AST coordinates are

$$1/a_j + 1/b_j, \quad e_j \cos\delta''_j, \quad e_j \sin\delta''_j, \quad n'_{j1}, \quad n'_{j2}, \ \xi''_j(t).$$

- For $t = 0$ these coordinates give a representation of the initial point cloud. For a wide range of circumstances (different values of e and different initial variances in ECI coordinates) they will be approximately Gaussian for $t = o$ and remain approximately Gaussian for $t > 0$. In particular, their behavior does not depend on the inclination angle of the central state.
- In Keplerian dynamics, the first five AST coordinates remain fixed under propagation. Only the mean anomaly changes; both the location and the spread of the point cloud for mean anomaly increase with time.
- In perturbed dynamics, the first five coordinates vary slowly with time.

III. Point Cloud Propagation in Different Coordinate Systems

Example 1. To illustrate the behavior of the different coordinate systems under propagation, consider an orbital object (eccentricity = 0.72 and orbital period = 628 minutes) whose initial state in Cartesian-ECI coordinate system is uncertain, with standard deviation = 10 km for each location coordinate and 0.2 km/sec for each velocity coordinate, where the uncertainties in all 6 coordinates are independent. The state of the object has been propagated for 20.2 days (approximately 46.31 orbits for the central state) following Keplerian dynamics, and the uncertainty in the final state has been summarized with 6-dimensional pairs plots in different coordinate systems. This example has been chosen to highlight non-normal behavior in the standard coordinate systems and also to confirm approximately normal behaviour in the AST coordinates system.

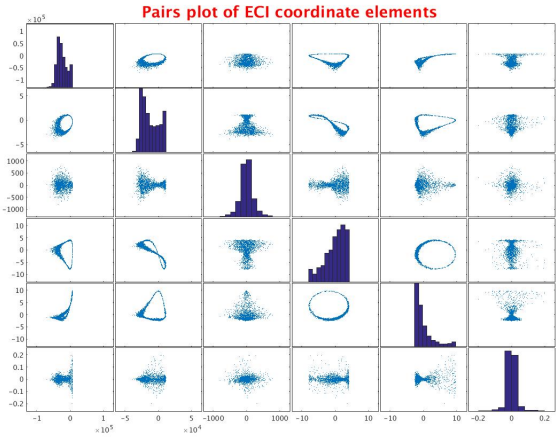

Fig. 2. **Example-1:** Propagated point cloud ($N = 2000$) in ECI coordinates for the three position and three velocity coordinates.

(a) In **ECI coordinates** (Fig. 2), all the bivariate scatter plots exhibit extreme non-normal behaviour.

(b) In **Keplerian coordinates** (Fig. 3), element 3 (inclination angle) is skew (a bounded range issue since the lower limit of the inclination angle is 0^o), and elements 4 and 5 are angles showing bimodal behavior. The scatter plots in the final column show a superimposition of a concentrated circular cluster and a longer thinner elliptical cluster; this is a winding number problem.

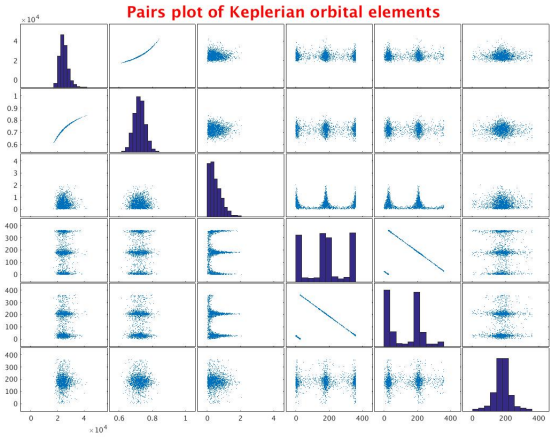

Fig. 3. **Example-1:** Propagated point cloud ($N = 2000$) in Keplerian coordinates.

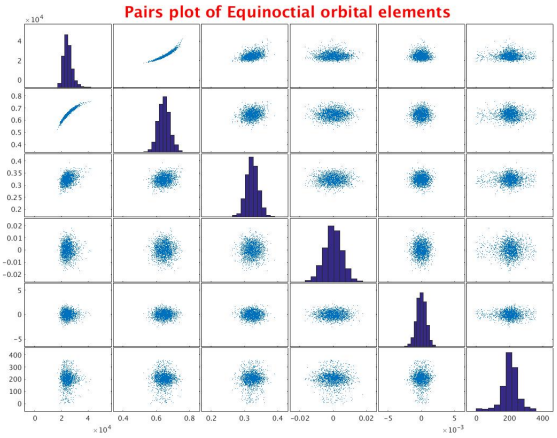

Fig. 4. **Example-1:** Propagated point cloud ($N = 2000$) in equinoctial coordinates

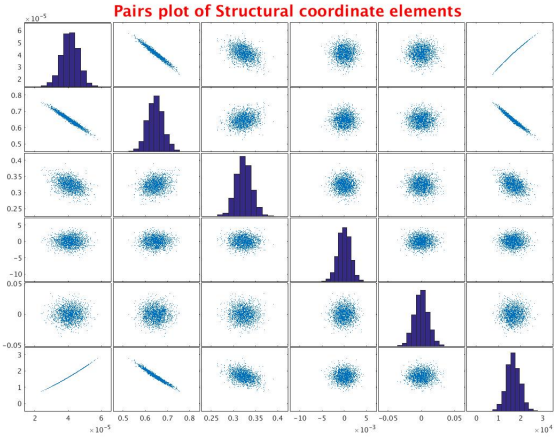

Fig. 5. **Example-1:** Propagated point cloud ($N = 2000$) in AST coordinates.

(c) In **Equinoctial coordinates** (Fig. 4), element 1 (length of the major axis) is skewed. The scatterplot of element 1 vs. element 2 shows some curvature. The scatter plots in the final column have the same problem as for Keplerian coordinates.

(d) In **AST coordinates** (Fig. 5), all the elements are approximately normally distributed.

To summarize, ECI and Keplerian coordinates are not useful for propagation as they often exhibit extreme non-normal behavior. Further, ECI and Keplerian coordinates show noticeable curvature and non-normal behaviour even for a small propagation time with a moderate amount of initial uncertainty in position and velocity components [5]. Equinoctial coordinates are better, but still not as good as AST coordinates. AST coordinates preserve normality under a wide range of conditions for the size of the initial uncertainty, ellipticity and propagation time [5].

IV. Mixture Modeling in AST Coordinates

The main purpose behind the development of AST coordinates is to facilitate the tracking of space objects. Assume that the observations take the form of angles-only position measurements. Consider first the case of unambiguous custody. We propose using an unscented Kalman filter (UKF) [6] in AST coordinates. Each step of UKF-AST filter takes the following form.

(a) At time t_n, the uncertainly in the state is approximately normally distributed in AST coordinates. This distribution can be summarized using 13 sigma points.

(b) Each sigma point can be propagated to time t_{n+1} either using Keplerian dynamics, or incorporating perturbation effects.

(c) An angles-only observation is made at time t_{n+1}. The update step of the Kalman filter involves re-weighting the sigma points and summarizing the updated state distribution by a new multivariate normal distribution. In addition the central state for the AST representation is updated.

When object custody is ambiguous, some modification to this procedure is needed. Suppose an object can be associated with two or more objects in a catalog at time t_n. Then the state distribution at time t_n is a mixture of two multivariate normal distributions. Sigma points are constructed and propagated for each component of the mixture. The update step involves re-weighting the sigma points as before, after which the updated state distribution is approximated by a new mixture of two multivariate normal distributions.

Example 2. To illustrate the procedure consider a situation with two objects at time t_0. The first object is same as in the previous section (eccentricity = 0.72 and orbital period = 628 minutes). The second object is also located in a HEO orbit (eccentricity = 0.67 and orbital period = 542 minutes). The two normal directions to the orbital planes are assumed to be the same. The uncertainties are represented in ECI coordinates by isotropic normal distributions for position (standard deviation

= 20 km) and velocity (standard deviation = 0.1 km/sec). The initial state vectors are represented in ECI, Equinoctial and AST coordinates in Figs 6-8. In general the one-dimensional plots are either unimodal or bimodal, depending on the extent of overlap of initial conditions.

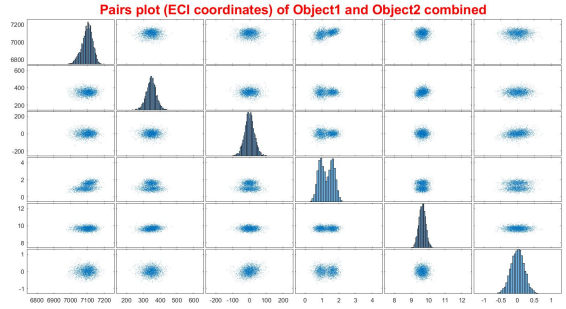

Fig. 6. **Example-2:** Initial point clouds ($N_A = 2000$ and $N_B = 2000$) for objects 1 and 2 represented in ECI coordinates.

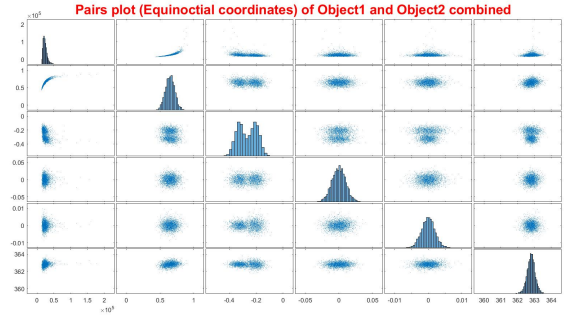

Fig. 7. **Example-2:** Propagated point clouds ($N_A = 2000$ and $N_B = 2000$) for objects 1 and 2 represented in Equinoctial coordinates.

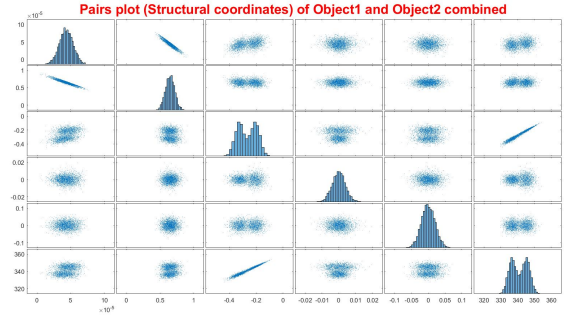

Fig. 8. **Example-2:** Propagated point clouds ($N_A = 2000$ and $N_B = 2000$) for objects 1 and 2 represented in AST coordinates.

Next consider what happens to the updated state distributions after two possible time intervals. In the first case an observation is made after 2 hours (Fig. 10); in the second case an observation is made after 21 hours (Fig. 11). The updated angles-only part of the state distributions are summarized in Figs. 10-11.

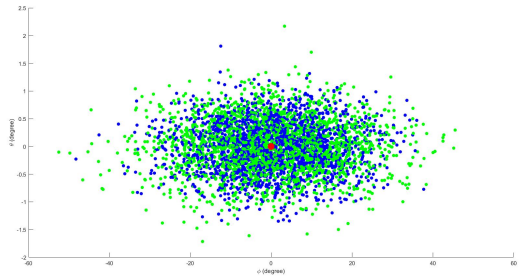

Fig. 9. **Example-2:** Angles-only representation of the point cloud at t = 0. The blue cluster indicates the distribution associated with the first object (A) and the green cluster represents the second object (B). The red dot is the central state. Note the high degree of overlap between the two distributions.

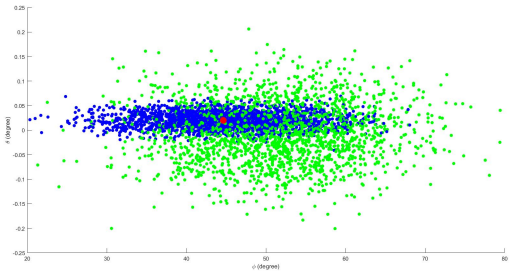

Fig. 10. **Example-2:** Updated angles-only state distribution for an observation after 2 hours. The point cloud for the first object (A) is represented using blue dots and for the second object (B) using green dots. The observation is represented by a red dot.

In Fig. 10, the angles-only state distributions after 2 hours are plotted. These distributions are highly overlapping and the object custody remains ambiguous. The posterior probabilities for the two groups are nearly equal, $p_A = 0.57,\ p_B = 0.43$).

In Fig. 11, the angles-only state distributions after 21 hours are plotted. These distributions are now well-separated and the object custody has now been resolved. The posterior probabilities for the two groups are now very different, $p_A = 1.000,\ p_B = 1e-21$).

V. Conclusion

In earlier work we showed how the standard coordinate systems were all unsuitable to a greater or lesser extent for the filtering problem. On the other hand, starting from an initial multivariate normal distribution in ECI coordinates, AST coordinates retain an approximate multivariate normal behavior after propagation in a wide variety of circumstances. Thus, when object custody is not ambiguous, it is straightforward to implement a version of the UKF in AST coordinates.

In this paper we have shown that the filtering methodology extends in a natural way to the setting where object custody is ambiguous. If an observation can be associated with one of J possible objects at an initial time, the initial uncertainty is now represented by a mixture of multivariate normal distributions with J equally likely components. Each component can be propagated separately. If the different objects have sufficiently

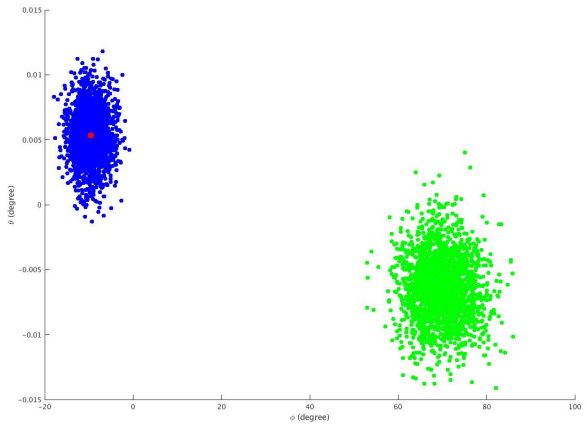

Fig. 11. **Example-2:** Updated angles-only state distribution for an observation after 21 hours. The point cloud for the first object (A) is represented using blue dots and for the second object (B) using green dots. The observation is represented by a red dot. The observation is now clearly associated with the object A.

different state distributions, the updated state distribution will eventually home in on the correct object.

ACKNOWLEDGMENT

This material is based upon work supported by the Air Force Office of Scientific Research, Air Force Materiel Command, USAF under Award No. FA9550-16-1-0099.

REFERENCES

[1] J. T. Kent, S. Bhattacharjee, I. I. Hussein, M. K. Jah, "Geometric restructurization of the space object tracking problem for improved uncertainty representation," 7th European Conference on Space Debris, Darmstadt, Germany, 2017.

[2] J. L. Junkins, M. R. Akella, K. T. Alfriend, "Non-Gaussian error propagation in orbital mechanics," Journal of the Astronautical Sciences, vol. 44, pp. 541–563, 1996.

[3] M. Valli, R. Armellin, P. D. Lizia, M. R. Lavgna, "Non linear mapping of uncertainties in celestial mechanics," Journal of Guidance,Control and Dynamics, vol. 36, pp. 48–63, 2013.

[4] J. T. Horwood, A. B. Poore, "Non linear mapping of uncertainties in celestial mechanics, Gauss von Mises distribution for improved uncertainty realism in space situational awareness," SIAM/ASA J. Uncertainty Quantification, vol. 2, pp. 276-304, 2014.

[5] J. T. Kent, S. Bhattacharjee, I. I. Hussein, M. K. Jah, "Nonlinear filtering using directional statistics for the orbital tracking problem with perturbation effects," Proceedings of the 28th AAS/AIAA Space Flight Mechanics Meeting, 2018.

[6] S. J. Julier, J. K. Uhlmann, "Unscented Filtering and Nonlinear Estimation," IEEE Proc., vol. 92, pp. 401–422, 2004.

[7] H. Curtis, "Orbital Mechanics for Engineering Students," Elsevier Aerospace Engineering Series, pp. 149–187, 2006.

[8] I. Park, D. J. Scheeres. "Hybrid method for uncertainty propagation of orbital motion," Journal of Guidance, Control, and Dynamics, Vol. 41, pp. 240–254, 2018.

[9] V. Vittaldev, R. P. Russell, and R. Linares, "Spacecraft uncertainty propagation using Gaussian mixture models and polynomial chaos expansions," Journal of Guidance, Control, and Dynamics, Vol. 39, pp. 2615–2626, 2016.

[10] G. R. Hintz, "Survey of orbit element sets," Journal of Guidance, Control, and Dynamics, Vol. 31, pp. 785–790, 2008.